Tidally Trapped Pulsations in HD 74423 discovered by TESS

G. Handler,[1] D. W. Kurtz,[2] S. A. Rappaport,[3] H. Saio,[4] J. Fuller,[5] D. Jones,[6,7] Z. Guo,[8] S. Chowdhury,[1] P. Sowicka,[1] F. Kahraman Aliçavuş,[1,9] M. Streamer,[10] S. J. Murphy,[11] R. Gagliano,[12] T. L. Jacobs[13] and A. Vanderburg[14,15]

[1] Nicolaus Copernicus Astronomical Center, Polish Academy of Sciences, ul. Bartycka 18, 00-716, Warsaw, Poland
[2] Jeremiah Horrocks Institute, University of Central Lancashire, Preston PR1 2HE, UK
[3] Department of Physics, and Kavli Institute for Astrophysics and Space Research, M.I.T., Cambridge, MA 02139, USA
[4] Astronomical Institute, Graduate School of Science, Tohoku University, Sendai 980-8578, Japan
[5] Division of Physics, Mathematics and Astronomy, California Institute of Technology, Pasadena, CA 91125, USA
[6] Instituto de Astrofísica de Canarias, E-38205 La Laguna, Tenerife, Spain
[7] Departamento de Astrofísica, Universidad de La Laguna, E-38206 La Laguna, Tenerife, Spain
[8] Department of Astronomy and Astrophysics, Pennsylvania State University, 421 Davey Lab, University Park, PA 16802, USA
[9] Çanakkale Onsekiz Mart University, Faculty of Sciences and Arts, Physics Department, 17100, Çanakkale, Turkey
[10] Research School of Astronomy and Astrophysics, Australian National University, Canberra, ACT, Australia
[11] Sydney Institute for Astronomy (SIfA), School of Physics, University of Sydney, NSW 2006, Australia
[12] Planet Hunters
[13] Amateur Astronomer, 12812 SE 69th Place Bellevue, WA 98006, USA
[14] Department of Astronomy, The University of Texas at Austin, 2515 Speedway, Stop C1400, Austin, TX 78712, USA
[15] NASA Sagan Fellow

It has long been suspected that tidal forces in close binary stars could modify the orientation of the pulsation axis of one or the other constituent stars (ref.[1]). Such stars have been searched for in the past, but so far never detected. Here we report the discovery of tidally trapped pulsations in the ellipsoidal variable HD 74423, containing a δ Scuti pulsator in a 1.6-d orbit with a low-mass companion star. The pulsating primary star is nearly filling its Roche lobe, and the pulsations have a much larger amplitude in one hemisphere. We interpret this as an obliquely pulsating distorted dipole oscillation with a pulsation axis aligned with the tidal axis. This is the first time such a phenomenon has been observed. It is unclear in which stellar hemisphere the oscillations are trapped because we cannot distinguish which of the two ellipsoidal light minima corresponds to viewing the L1 point. The answer lies in the nature and temperature of the secondary star that we could not detect. New radial velocity measurements will provide the solution. In the meantime, HD 74423 stands out as a unique laboratory in which the interactions of stellar pulsations and tidal distortion can be studied.

Much of the present-day understanding of the universe is rooted in the knowledge of the basic parameters and structure of the stars. The precise determination of these parameters rests on two methods: the analysis of eclipsing binary stars and asteroseismology. Whereas detached eclipsing binaries facilitate the determination of global stellar parameters to the highest precision (e.g., see ref.[2]), asteroseismology allows the determination of interior stellar structure to fine detail (ref.[3]). Thus, even more rewarding are asteroseismic analyses of the components of detached eclipsing binaries.

Proximity effects between binary star components can influence stellar oscillations. The modification of an interior stellar structure due to mass transfer can be traced asteroseismically. Many decades ago it was theoretically predicted that the excitation of stellar oscillations can be augmented by tides (ref.[4]), but convincing observational evidence has only been accumulated in the recent past (ref.[5]).

It was only with the advent of the *Kepler* space telescope that binary components whose oscillations were affected by tides were discovered in larger numbers. Most prominent among these are the highly eccentric binary "Heartbeat" stars (e.g., refs.[6,7,8,9]). Some of these stars show tidally excited gravity modes that are exactly resonant with high harmonics of the orbital frequency.

Aside from tidal excitation, it has been speculated (ref.[1]) that a binary companion could cause a tilt of the stellar pulsation axis, which would result in amplitude modulation of a nonradial pulsation over the orbit. This is quite analogous to what had already been observed in the rapidly oscillating Ap (roAp) stars (ref.[10]). In the latter case, however, it is the magnetic field of those stars that tilts the pulsation axis.

The roAp stars show high radial overtone, nonradial pulsation modes with frequency multiplets that have frequency separations exactly equal to the known rotation frequency for a particular Ap star, which is determined with precision from rotationally induced light

variations caused by long-lived abundance spots. In the asymptotic regime, ref.[11] showed that when $n \gg \ell$, where n is the radial overtone and ℓ is the spherical degree of a pressure (p) mode,

$$\omega_{\ell,m} = \omega_{\ell,0} + m(1 - C_{n,\ell})\Omega, \quad (1)$$

where ω is the pulsation frequency, Ω is the rotation frequency and $C_{n,\ell}$ is the 'Ledoux constant', which for p modes usually differs from zero by only a few per cent. Ref.[10] was able to show for the roAp stars that $C_{n,\ell}$ is zero, if the above equation is applied, and he proposed instead the oblique pulsator model, where the pulsation axis is the magnetic axis, which is known to be oblique to the rotation axis in most Ap stars. The roAp stars thus became the first pulsating stars where it could be shown that the pulsation axis was *not* the rotation axis. There were many subsequent developments of the oblique pulsator model, and it is now believed that the pulsation axis is neither the magnetic axis, nor the rotation axis, but rather lies along a plane between those (ref.[12]).

With it being clear from the roAp stars that nonradially pulsating stars can have pulsation axes other than the rotation axis, an obvious idea is that in close binary stars, the tidal distortion may not only tilt the pulsation axis as suggested by ref.[1], but even be sufficient to make the line of apsides the pulsation axis. Refs.[13,14] also considered this possibility. Searches for this new type of obliquely pulsating stars have been ongoing with high precision *Kepler* mission data, and now with the new *TESS* data. However, no pattern of frequencies typical of oblique pulsation, as in the roAp stars, was found - until now!

HD 74423 is a $V = 8.61$ mag A-type star in the Southern Hemisphere for which there is little information in the literature. Ref.[15] gave a spectral type of A1V. Four decades later, ref.[16] reported photometric variability with a period of 0.79037(1) d and a peak to peak amplitude of 0.08 mag found in ASAS-3 data (ref.[17]). On this basis, they classified HD 74423 as a candidate photometrically variable chemically peculiar star. We list the known properties of this star in Table 1.

It comes as a surprise in this picture that ref.[18] reported HD 74423 as a chemically peculiar star of the λ Bootis type, with a spectral type of A7V kA0mA0, and determined $T_{\rm eff} = 8100$ K, $\log g = 3.6$, $[M/H] = -1$ and $E(B-V) = 0.055$, consistent with this classification. The chemical peculiarity of λ Bootis stars is believed to stem from accretion of metal-depleted gas from either the interstellar medium or from a circumstellar disk or shell (ref.[19]). Because searches for magnetic fields in λ Bootis stars (ref.[20]) have not yielded positive results to date, the current understanding is that, unlike the roAp stars, λ Bootis stars do not have surface spots. Therefore, the possible presence of rotational variability of this star is suspect, and we show below that HD 74423 instead exhibits binary ellipsoidal light variations.

Observations and their analysis

The peculiar pulsation pattern in HD 74423 = TIC 355151781 was first noticed as being quite unusual by two of us (R. G. and T. J) during visual surveys of the *TESS* light curves

Table 1: Properties of the HD 74423/TIC 355151781 System

Parameter	Star
RA (J2000) (deg)	130.07484
Dec (J2000) (deg)	−64.83796
T^a	8.358 ± 0.017
G^b	8.562 ± 0.001
${G_{\rm BP}}^b$	8.692 ± 0.003
${G_{\rm RP}}^b$	8.367 ± 0.003
J^c	8.065 ± 0.020
H^c	8.021 ± 0.067
K^c	7.944 ± 0.040
$W1^d$	7.891 ± 0.027
$W2^d$	7.917 ± 0.020
$W3^d$	7.919 ± 0.018
$W4^d$	7.816 ± 0.105
$E(B-V)$ (mag)^e	0.055
$T_{1,\rm eff}$ (K)^f	8050 ± 150
R_1 $(R_\odot)^f$	4.7 ± 0.2
M_1 $(M_\odot)^f$	2.3 ± 0.2
L_1 $(L_\odot)^f$	83 ± 4
Orbital Period (d)^f	1.5807233 ± 0.0000015
Distance (pc)^b	491 ± 8
μ_α (mas yr^{-1})^b	-9.8 ± 0.07
μ_δ (mas yr^{-1})^b	$+11.7 \pm 0.07$

Notes. (a) TESS Input Catalog. (b) Gaia DR2 (ref.[41]). (c) 2MASS catalog (ref.[42]). (d) WISE point source catalog (ref.[43]). (e) (Ref.[18]). (f) This work.

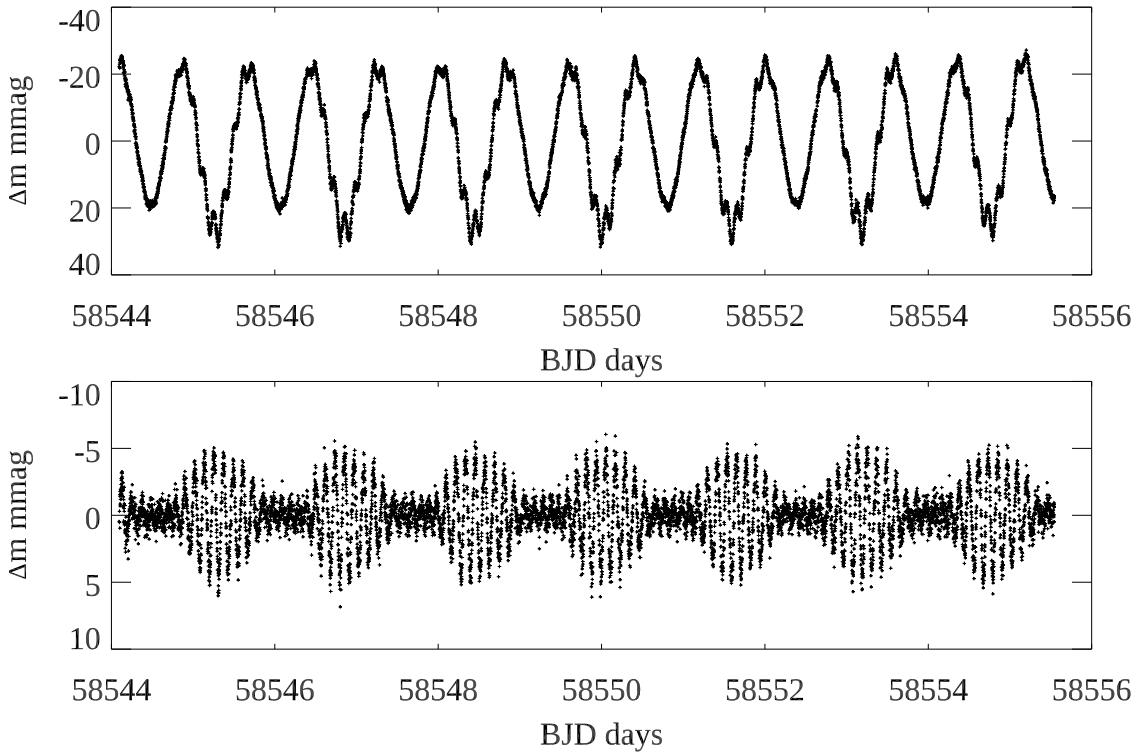

Figure 1: Top: A section of the *TESS* light curve of HD 74423 showing the clear ellipsoidal light variations, along with higher frequency pulsations. The sections of the light curve not shown are similar. Bottom: The same section of the light curve after pre-whitening the orbital variations and low frequency artefacts. The modulation of the pulsation amplitude with the orbital period is striking.

from Sector 9. Such visual surveys have led to the discovery of a number of unusual and interesting astronomical objects not picked up by standard Box Least Squares ('BLS'; ref.[21]), searches for periodic signals. Examples of these discoveries are listed in Sect. 2.2 of ref.[22]. HD 74423 was ultimately observed by *TESS* during Sectors 9, 10, and 11 in 2-min cadence.

The top panel of Fig. 1 shows a section of the initial light curve (the full light curve would be too compressed at this scale to see the details) where the variations already reported by ref.[16] are obvious. However, the light curve shows minima of alternating depth whereas the maxima do not alternate. This type of light curve is characteristic for an ellipsoidal variable (ref.[23]) and less reminiscent of a rotational variable as implied by ref.[16]. The differing minima arise, in part, from differential gravity darkening near the L1 and L2 points of the tidally distorted star. In the lower panel of Fig. 1, the orbital variability has been removed, which shows that the amplitude of the pulsation is clearly modulated with the orbit.

The amplitude changes by about a factor of 10 between the two ellipsoidal light minima. Obscuration of the pulsating star by the companion cannot explain this modulation, as it would also cause eclipses of at least 0.7 mag depth, which are not seen. We therefore face the curious situation that the pulsations are apparently mostly confined to one hemisphere of the star.

The *TESS* data have a time span of 79.8 d with a centre point in time of t_0 = BJD 2458583.99411, and comprise 50146 data points after a few outliers were removed following an inspection by eye. This t_0 was used to begin the analysis, but later changed to the time of rotational light extremum, and to test the oblique pulsator model. For the assessment of phase errors with nonlinear least-squares fitting, it is important that the t_0 chosen is near to the centre of the data set. Since frequency and phase are degenerately coupled in the fitting of sinusoids, when t_0 is not the centre of the data set, small changes in frequency result in very large changes in phase, since phase is referenced from t_0.

The top panel of Fig. 2 shows the initial amplitude spectrum, where the second harmonic of the orbital frequency is the highest peak, as we expect for a double-wave, ellipsoidal light curve in a close binary. The derived orbital frequency is $\nu_{\rm orb} = 0.6326218 \pm 0.0000006\,{\rm d}^{-1}$ ($P_{\rm orb} = 1.580723 \pm 0.000002\,{\rm d}$). This derivation is made from data with the pulsation frequencies removed, so that they do not contribute to the error calculation for the orbital frequency.

The second panel of Fig. 2 shows the amplitude spectrum of the residuals after a five-harmonic fit of the orbital variation $\nu_{\rm orb}$ has been removed from the data. The pulsation multiplet and two of its harmonic multiplets are visible in this panel, as are low frequency peaks that are instrumental artefacts. We removed those low frequency artefacts with a high-pass filter to produce the amplitude spectrum in the third panel, which shows only the pulsation frequency and harmonics along with their orbital sidelobes. The purpose of removing the low frequency artefacts was to obtain better error estimates that do not contain instrumental variance.

From the third panel in Fig. 2, it is apparent that most of the pulsational variation is represented by a frequency multiplet centred on the highest peak. By extracting the frequencies in this multiplet and examining their frequency separations, it is apparent that all are separated within the errors by the orbital frequency, $\nu_{\rm orb} = 0.6326218 \pm 0.0000006\,{\rm d}^{-1}$. There is, therefore, only one pulsation frequency, $\nu_1 = 8.756917 \pm 0.000010\,{\rm d}^{-1}$, and its orbital sidelobes and harmonics.[1] The harmonic multiplets are likewise separated by $\nu_{\rm orb}$. We therefore used a combination of linear and nonlinear least-squares fitting to optimise our determinations of the frequencies, amplitudes and phases for the multiplets. Table 2 shows the results of those procedures. The phases of the pulsation frequency and its first sidelobes are very close to equal at the time when the line of sight is along the orbital line of apsides. This is a clear signature of oblique pulsation along that axis. We note that the frequency ratio of the pulsation frequency to the orbital frequency is 13.84226 ± 0.00003, which is nearly $6000\,\sigma$ away from an integer, hence the pulsation is not in tidal resonance.

Finally, we fitted the pulsation frequency $\nu_1 = 8.756917\,{\rm d}^{-1}$ by least-squares to sections of the data 0.1-d long to examine the amplitude and phase variations over the orbital cycle. We also binned the original light curve by a factor of 100 – i.e., into 200-min time bins – and plot all three curves in Fig. 3. This figure shows that orbital light minimum and pulsation maximum coincide at the time when the line of sight is along the line of apsides.

[1] The amplitude of signal $\nu_1 - \nu_{\rm orb}$ is similar to that of ν_1 itself which makes it another candidate to be the actual pulsation frequency. However, the presence of the second harmonic triplet that is symmetric around $3\nu_1$ clearly argues against that hypothesis.

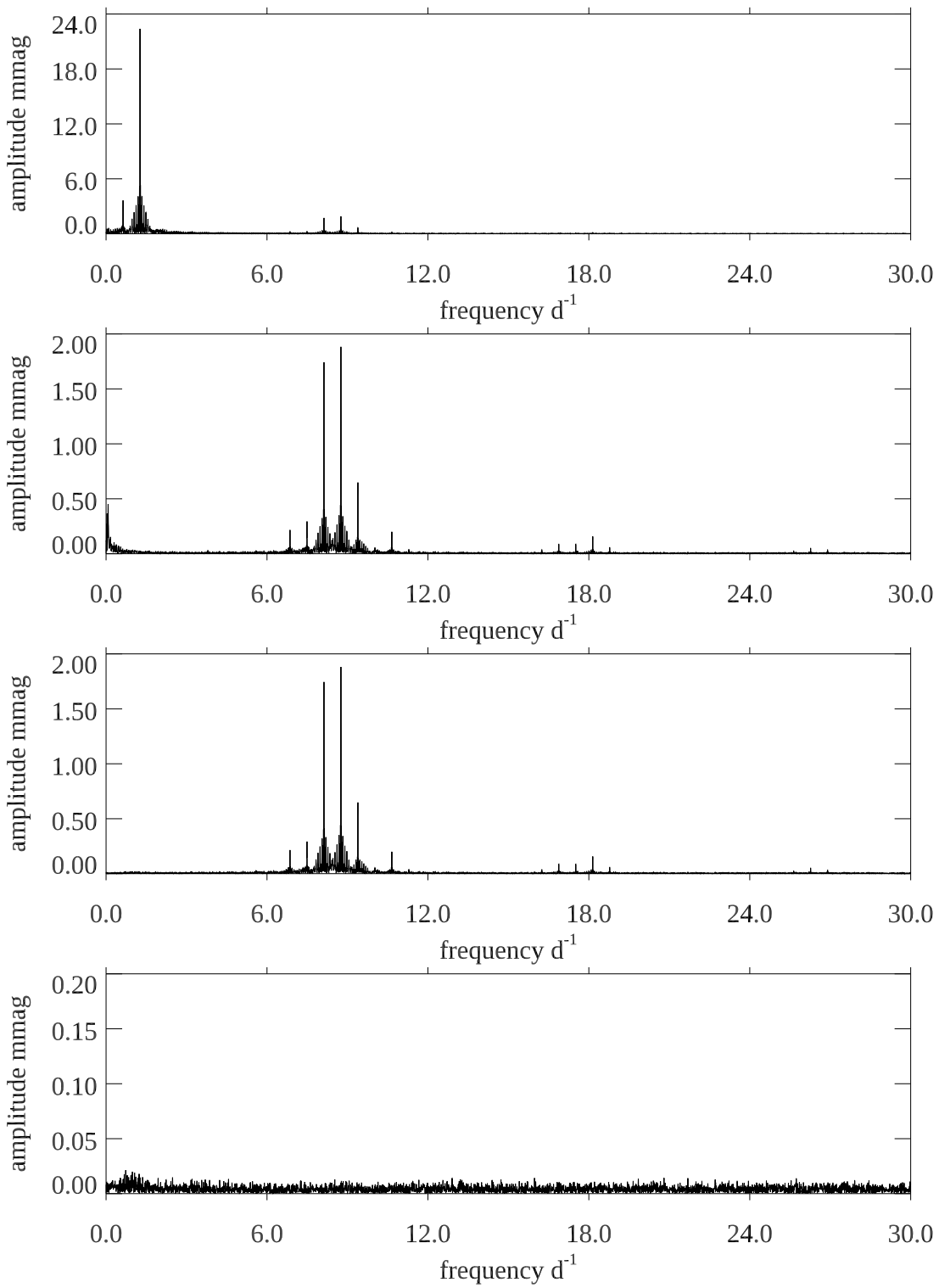

Figure 2: Top: The initial Fourier amplitude spectrum of the light curve of HD 74423, where the highest peak is at twice the orbital frequency, $\nu_{\rm orb} = 0.6326218 \pm 0.0000006\,{\rm d}^{-1}$. Second panel: The amplitude spectrum of the residuals after pre-whitening a harmonic series of five terms based on the orbital frequency. It can be seen that there are low frequency peaks, which are instrumental artefacts. The pulsation multiplet centred around $\nu_1 = 8.756917 \pm 0.000010\,{\rm d}^{-1}$ and its harmonics are visible. The third panel shows the same as the second, but after a high-pass filter has removed the low-frequency artefacts. The multiplets can easily be seen. The bottom panel shows the amplitude spectrum of the residuals after the fit shown in Table 2. Note the changes in ordinate scale.

Table 2: A least squares fit of the frequency multiplets for ν_1 and its harmonics. The zero point for the phases, t_0 = BJD 2458584.78684, has been chosen to be a time when the two first orbital sidelobes have equal phase; note that those are both -1.833 rad, and the phase of ν_1 is close to these. This choice is independent of the orbital variations, but notice the orbital phase for comparison. It can be seen that orbital light minimum coincides with pulsation maximum, as expected in the oblique pulsator model.

	frequency d^{-1}	amplitude mmag ± 0.004	phase radians
$\nu_1 - 5\nu_{\rm orb}$	5.593807	0.032	-1.100 ± 0.119
$\nu_1 - 4\nu_{\rm orb}$	6.226429	0.017	1.736 ± 0.216
$\nu_1 - 3\nu_{\rm orb}$	6.859051	0.228	1.985 ± 0.017
$\nu_1 - 2\nu_{\rm orb}$	7.491673	0.292	-1.751 ± 0.013
$\nu_1 - \nu_{\rm orb}$	8.124295	1.757	-1.833 ± 0.002
ν_1	8.756917	1.894	-2.129 ± 0.002
$\nu_1 + \nu_{\rm orb}$	9.389539	0.656	-1.833 ± 0.006
$\nu_1 + 2\nu_{\rm orb}$	10.022161	0.057	1.427 ± 0.066
$\nu_1 + 3\nu_{\rm orb}$	10.654783	0.195	-1.524 ± 0.019
$\nu_1 + 4\nu_{\rm orb}$	11.287405	0.039	-1.562 ± 0.096
$\nu_1 + 5\nu_{\rm orb}$	11.920027	0.012	2.125 ± 0.309
$2\nu_1 - 2\nu_{\rm orb}$	16.248589	0.036	-0.077 ± 0.105
$2\nu_1 - \nu_{\rm orb}$	16.881211	0.090	-1.082 ± 0.042
$2\nu_1$	17.513833	0.086	2.381 ± 0.043
$2\nu_1 + \nu_{\rm orb}$	18.146455	0.157	2.467 ± 0.024
$2\nu_1 + 2\nu_{\rm orb}$	18.779077	0.060	2.555 ± 0.062
$3\nu_1 - \nu_{\rm orb}$	25.638128	0.025	-1.822 ± 0.151
$3\nu_1$	26.270750	0.053	-1.482 ± 0.071
$3\nu_1 + \nu_{\rm orb}$	26.903372	0.038	-1.638 ± 0.098

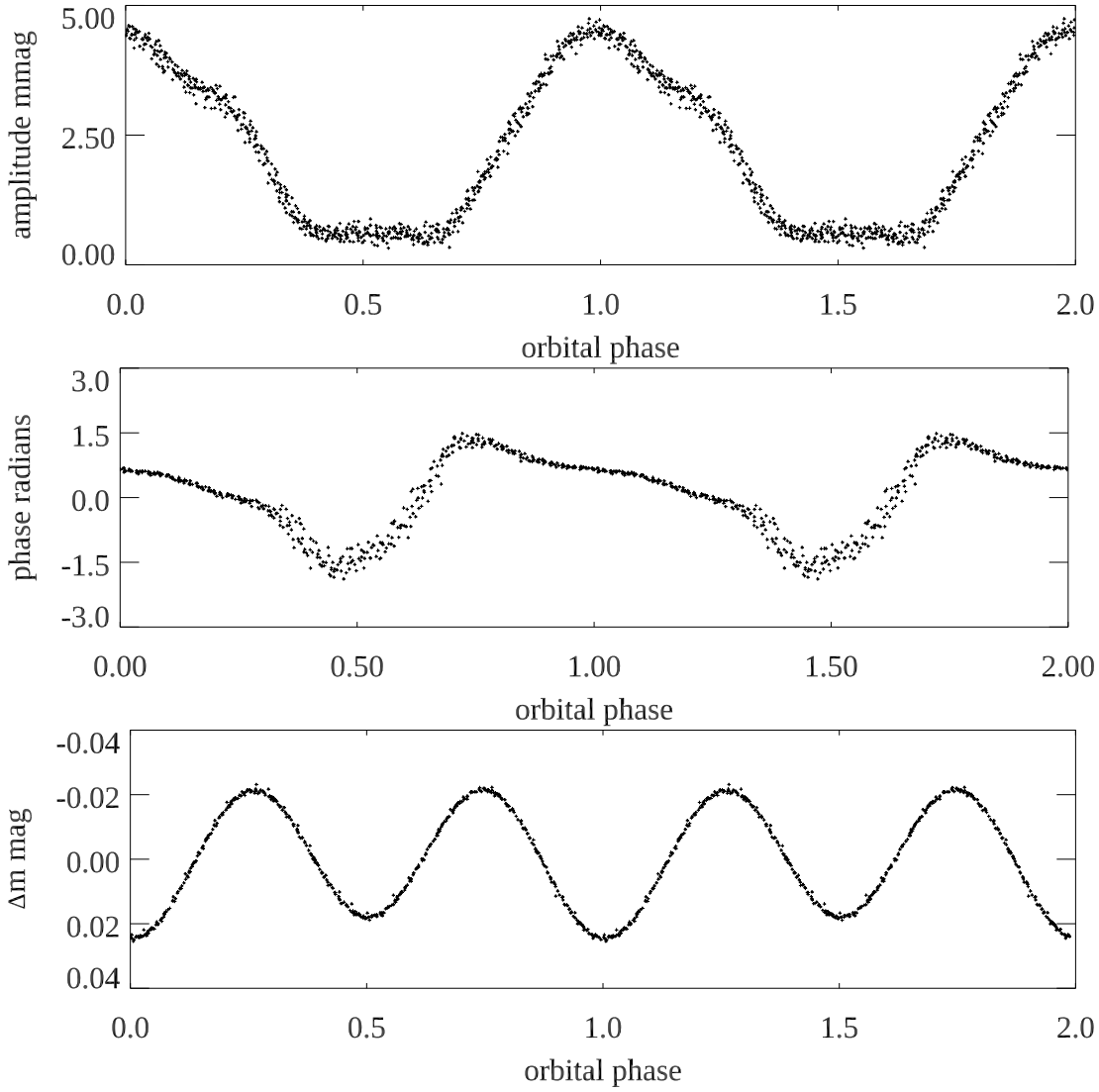

Figure 3: Top: The pulsation amplitude variation as a function of orbital phase taking the $8.756917\,\mathrm{d}^{-1}$ frequency to be the pulsation frequency. The zero point in time is t_0 = BJD 2458584.78684, which was chosen to set the two first orbital sidelobes to have equal phase. That coincides with pulsation amplitude maximum, as expected for an oblique pulsator. Middle: the pulsation phase variation over the orbital cycle with a range of 2π radians. The quicker phase reversals come at amplitude minimum. Bottom: the orbital light variations as a function of orbital phase for comparison. The data have been binned to 200-s, and the pulsation variations have been removed. It can be seen that orbital light minimum coincides with pulsation maximum, as expected in the oblique pulsator model.

There is, in principle, a small contribution to the multiplet sidelobes because of the frequency variation caused by the orbital motion (Doppler shift) known as frequency modulation (FM). The relative amplitudes of the first sidelobes compared to that of the central frequency for this effect is given by equation 21 of ref.[24] (note, however, that there its a typographical error in that equation; the first term should be $(2\pi G)^{\frac{1}{3}}/\mathrm{c}$). Applying the correct form of that equation gives their factor $\alpha \sim 0.001$. That is, the sidelobes generated by the frequency modulation are only 1/1000 the amplitude of the central peak, and this is negligible in our case here – being only half of the error in the amplitude determination – and can be ignored.

We have tried to fit the variation of the pulsation amplitude and phase over the orbit in analogy to magnetically modulated variability in the roAp stars. We assume luminosity variations arise from the temperature variation δT on the stellar surface, which can be decomposed into spherical harmonics

$$\delta T \propto e^{i\omega t} \sum_{\ell=0}^{2} A_\ell Y_\ell^0(\theta_\mathrm{p}, \phi_\mathrm{p}), \tag{2}$$

where $(\theta\mathrm{p}, \phi_\mathrm{p})$ represent spherical coordinates whose axis aligns with the line of apsides; i.e., we assume the pulsation is axisymmetric about the tidal axis. Converting the coordinate $(\theta_\mathrm{p}, \phi_\mathrm{p})$ to the coordinate whose axis is the rotation axis, and to the inertial coordinate whose axis is along the line of sight, and then integrating the visual hemisphere at each epoch, we obtain the luminosity variation as a function of time as

$$\Delta L(t) \propto e^{i\omega t} \sum_{\ell=0}^{2} \sqrt{2\ell+1} A_\ell \sum_{m=-\ell}^{\ell} d^\ell_{m,0}(\beta) d^\ell_{0,m}(i_o) e^{-im\Omega t} \tag{3}$$

where the coefficients $d^\ell_{m,0}(\beta)$ and $d^\ell_{0,m}(i_o)$ arise in converting the coordinate $(\theta_\mathrm{p}, \phi_\mathrm{p})$ to the one associated with the rotation axis (the pulsation axis is inclined to the rotation axis by β) and to the coordinate axis associated with the line of sight (the line of sight is inclined to the rotation axis by angle i_o (see e.g., refs.[25,26] for details).

We have assumed $\beta = 90°$ for a pulsation axis in the orbital plane, and have also assumed an inclination angle $i_o = 40°$. We then searched for a set of amplitude ratios $(A_1, A_2)/A_0$ (which are complex numbers in general) to best reproduce the observed amplitude and phase modulation of HD 74423 (Fig. 3). The best-fit model was obtained with $A_1/A_0 = (-1.3, -0.4i)$ and $A_2/A_0 = (1.0, 0.0i)$. The amplitude and phase modulations and amplitudes of sidelobes are compared with the observed ones in Fig. 4. Except at the orbital phase of 0.3 and 0.7, the phase and amplitude variability are reasonably reproduced, showing the pulsation is largely confined to one hemisphere. The deviations between our fit and the data cannot be avoided if we adopt an axisymmetric eigenfunction with respect to the pulsation axis, so it is clear that the pulsation is not exactly aligned with the tidal axis. The modelled surface amplitude distribution of the pulsation is shown in Fig. 5, again showing the higher amplitude near the tidal axis.

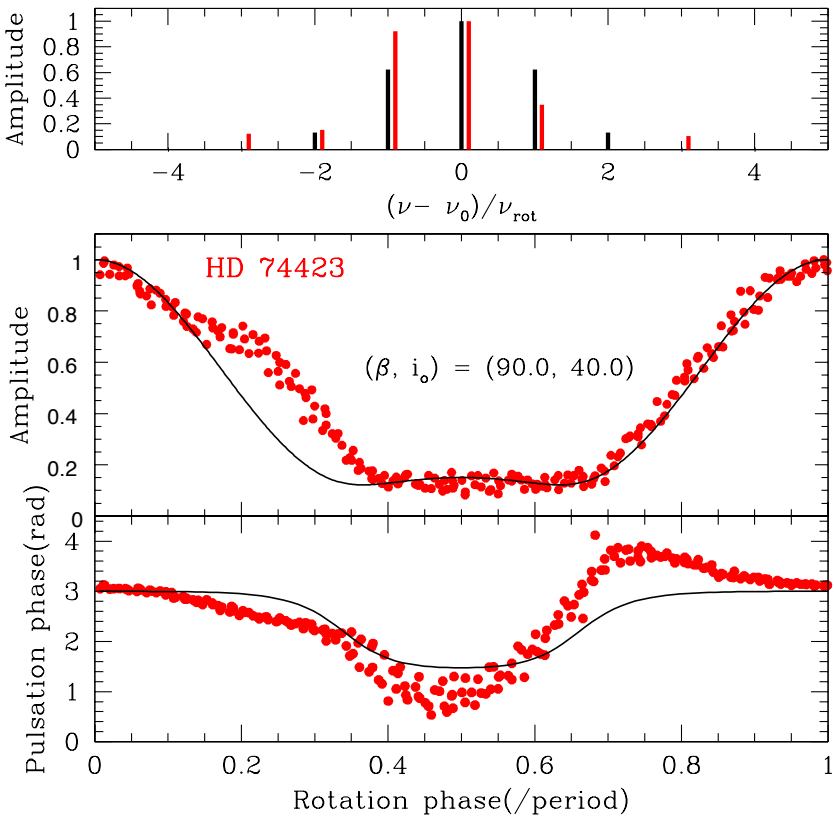

Figure 4: Top: comparison of the multiplet amplitudes (red lines) and those of our best-fit model (black lines) normalised by the amplitude of the central frequency. Middle: amplitude modulation of HD 74233 (red dots) compared with the model (black lines). Bottom: same comparison, but for the phase modulation.

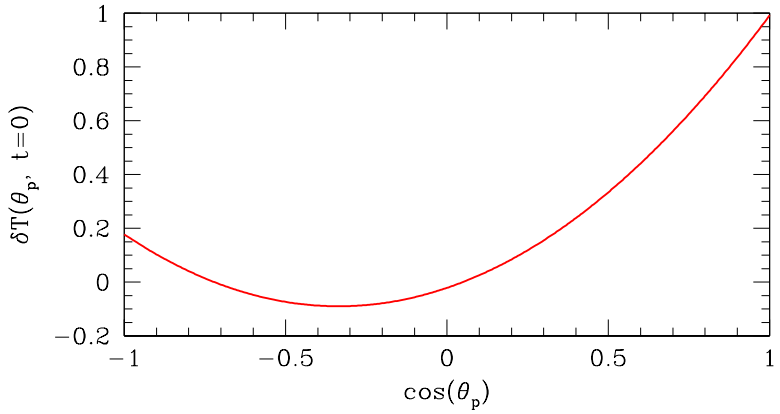

Figure 5: Temperature perturbation at the initial pulsation phase as a function of $\cos\theta_p$. This asymmetric distribution is required to reproduce the run of the pulsation amplitude in Fig. 4 and indicates the pulsation amplitude to be trapped in one hemisphere.

Table 3: Radial velocity measurements of HD 74233. The orbital phases were computed with respect to ellipsoidal variability light minimum. The error estimates are purely internal, hence the accuracy of the radial velocities could be poorer by up to a factor of three given the low resolution of our spectra.

HJD - 2450000 d	Orbital phase	RV (barycentric) km s^{-1}
8628.23500	0.4849	$+12.1 \pm 1.6$
8629.24683	0.1249	$+10.8 \pm 1.2$
8631.22027	0.3735	$+24.2 \pm 1.5$

Spectroscopy and SED fitting

From low-resolution spectroscopy (see methods section) we derive $T_{\rm eff} = 8000 \pm 150$ K, $[M/H] = -1.5 \pm 0.1$ and $v \sin i < 60\,{\rm km\ s^{-1}}$. This is not significantly different from the values derived by ref.[18]. Hence we adopt the mean of the two determinations (8050 ± 150 K) as the final value. That HD 74423 is a λ Bootis star implies that its surface abundances do not reflect its interior chemical composition. The star is not overall metal-poor, as demonstrated by the presence of a number of carbon lines not reproduced by a stellar atmosphere with $[M/H] = -1.5$. We therefore confirm HD 74423 as a λ Bootis type star, and show part of the analysis in Fig. 6. No evidence for the presence of a secondary spectrum was found.

We list radial velocities derived from our spectra in Table 3. The radial velocity measured during the last night is significantly different from the others, suggesting the presence of orbital motion due to a companion, as expected for an ellipsoidal variable. However, the RV points are too few in number and low in accuracy to allow for a meaningful orbital phase and amplitude to be determined.

If the secondary star contributes sufficiently to the total luminosity of the system and has a temperature significantly different from that of the primary, it may be detected via excess flux in the infrared or ultraviolet. To this end, we have collected archival fluxes of the HD 74423 system in all available passbands. As a result, we obtained an SED $T_{\rm eff} = 7780 \pm 255$ K, in reasonable agreement with the spectroscopy. Figure 7 shows the outcome of this procedure.

There is no evidence for excess flux due to the companion, in either the infrared or in the ultraviolet. The only striking feature is that the near-ultraviolet Galex flux is considerably lower than expected from the model flux, whereas the far-ultraviolet flux is very well matched. We have no astrophysical explanation for this observation.

Basic stellar parameters

The Gaia DR2 parallax of HD 74233 is 2.04 ± 0.03 mas. With $V = 8.61$ mag and $E(B-V) = 0.055$ mag (Table 1), $A_v = 3.2E(B-V)$, this results in $M_v = -0.02 \pm 0.04$ mag. With the bolometric correction taken from ref.[27] we arrive at $M_{\rm bol} = -0.05 \pm 0.04$ mag, and with $M_{\rm bol} = 4.74$ mag for the Sun (ref.[28]), we obtain $\log L/L_\odot = 1.92 \pm 0.02$. Assuming $T_{\rm eff} = 8050 \pm 150$ K (Table 1) yields $R = 4.66 \pm 0.18\,{\rm R}_\odot$.

Figure 8 shows a comparison of these parameters with theoretical stellar evolution tracks, computed with the MESA stellar evolution code (ref.[30]) using a solar metallicity of $Z =$

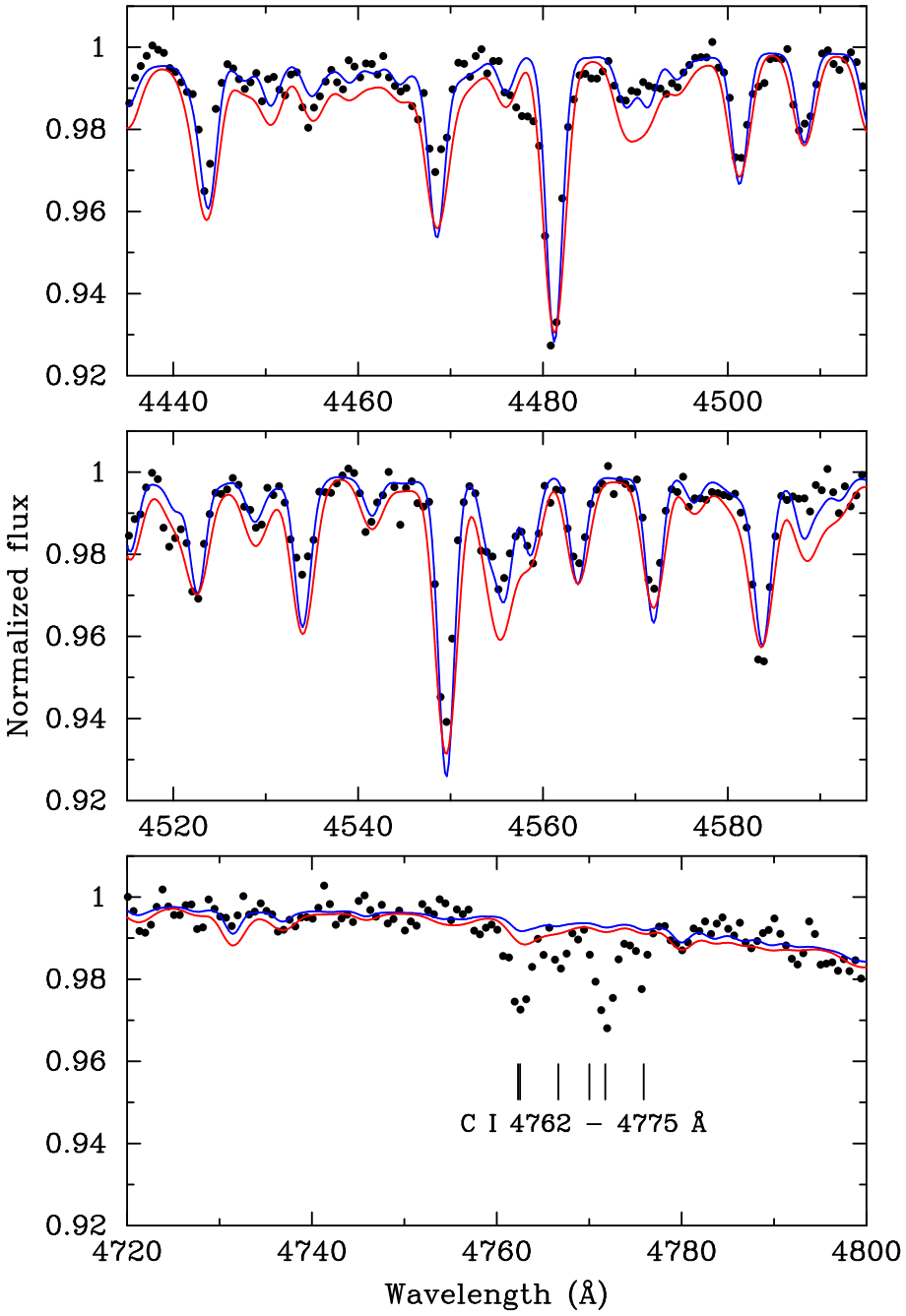

Figure 6: Selected parts of the averaged metallic-line spectrum of HD 74423 obtained on 2019 May 24 (S/N $\approx$ 350.) The observations are shown as black dots. The blue line represents a model atmosphere fit with $\log g = 3.5$, $T_{\rm eff} = 8000$ K, $[M/H] = -1.5$, and $v \sin i = 0$ km s^{-1} . The red line shows a model atmosphere fit with the same $\log g$ and $T_{\rm eff}$, but $[M/H] = -1.3$ and $v \sin i = 100$ km s^{-1}. Top two panels: rotation with $v \sin i = 100$ km s^{-1} is not consistent with the observations, as it results, e.g., in a poor fit of the line blends near 4515, 4530 and 4555 Å or the single lines 4445 and 4585 Å. Bottom panel: $[M/H] = -1.5$ cannot explain the strength of the CI $4762 - 4775$ Å multiplet, corroborating that HD 74423 has abundance anomalies of the λ Bootis type.

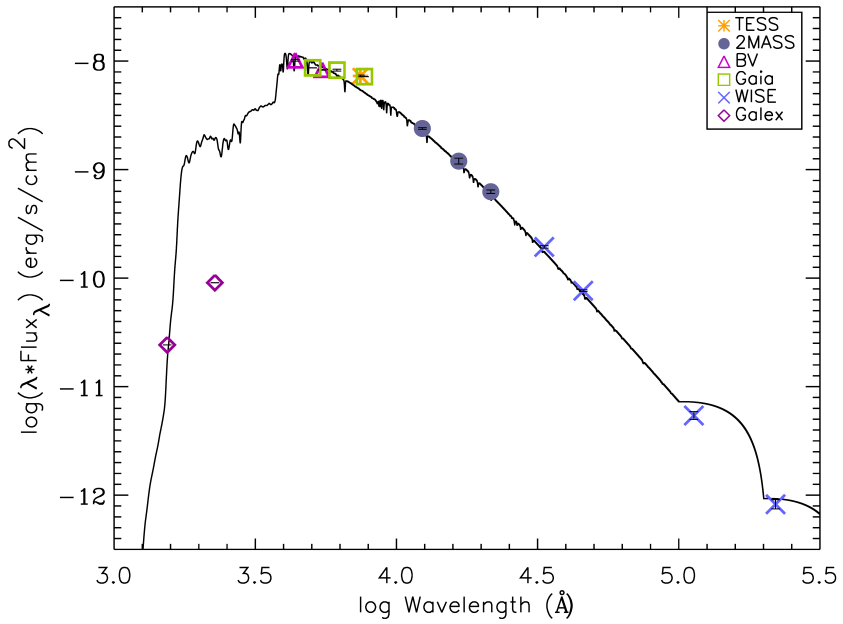

Figure 7: Spectral energy distribution of HD 74423 compared to a Kurucz model atmosphere.

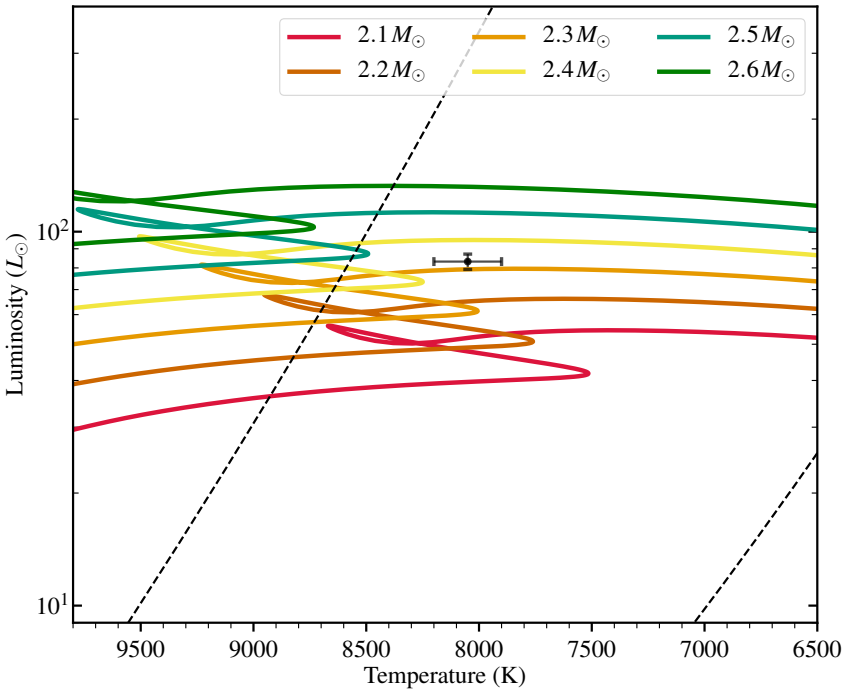

Figure 8: The position of HD 74423 (full circle with error bar) in a theoretical HR diagram. Model evolutionary tracks (full lines) are labeled with their masses. The boundaries of the δ-Scuti instability strip (ref.[29]) are shown with dotted lines.

0.0126 (ref.[31]). The models include moderate overshoot (exponential overshoot parameter $f = 0.02$) and rotational mixing, and are initialized with rotational velocities of 50 km s^{-1} at the ZAMS. These models suggest $M = 2.33 \pm 0.03\,\mathrm{M}_{\odot}$, but the measurement error is likely to be far smaller than the uncertainties associated with the stellar models - and our neglect of the secondary's contribution to the total light. A different rotational velocity or metallicity would add much larger systematic contributions of a few tenths of a solar mass. The primary lies near the terminal age main-sequence (TAMS), though it is not clear whether it has exhausted hydrogen in its core. In any case, with the mass and radius thus determined, we confirm that $\log g = 3.47 \pm 0.04$ and derive the pulsation constant $Q = P\sqrt{\bar{\rho}/\bar{\rho}_{\odot}}$, where P is the pulsation period and $\bar{\rho}$ is the mean stellar density. For the single pulsation frequency we find $Q = 0.017 \pm 0.001$ d, which is expected for δ Scuti pulsation near the hot border of the instability strip (ref.[32]). This Q value is consistent with that of the third radial overtone (ref.[33]). However, given the evolutionary state of the star, it would most likely be a high-order mixed mode if nonradial, with the major contribution to mode energy stemming from the g-mode cavity.

Modelling the ellipsoidal variations

Using the `PHOEBE` code (see methods section), the overall amplitudes of the ellipsoidal light variation could be reproduced for a range of inclinations ($45^{o} \lesssim i \lesssim 55^{o}$) and mass ratios ($0.05 \lesssim q \lesssim 0.10$). However, we were unable to reproduce precisely the shape of the observed light curve and, in particular, the orbital phases of the observed maxima. There are several possible explanations for this, the most likely being that the assumed gravity darkening (β=1.0, as is typically assumed for radiative stars) and limb darkening coefficients (interpolated from the model atmospheres of ref.[34] following the scheme outlined in ref.[35]) are not valid for the system. However, we cannot exclude the more intriguing possibilities that the orbit is slightly eccentric ($e \sim 0.03$), that one hemisphere of the primary is partially covered by a "spot" which modifies its luminosity (beyond that expected by gravity darkening), or that the secondary is itself close to Roche lobe filling (where partial eclipses of the extended "neck" of the primary by the inflated secondary could contribute to the observed light curve morphology even though the light contribution of the secondary would be minimal compared to the much larger primary). It must be stressed, however, that a trial-and-error exploration of the additional parameter space opened up by entertaining these possibilities similarly failed to bear fruit with no combination being found that could adequately reproduce the entirety of the light curve.

Under the assumption that the secondary is a cool object, e.g. a normal main sequence star, the deeper minimum of the ellipsoidal variations – during which the pulsation amplitude is much larger – corresponds to the L1 point of the orbit facing the observer, i.e. when the more gravity-darkened hemisphere of the primary faces the observer. However, if the secondary is sufficiently hot that it irradiates the gravity-darkened neck of the primary star, the deeper ellipsoidal light minimum may actually correspond to the orbital L2 point facing the observer. In other words, there is an ambiguity in which of the primary's hemispheres the oscillations are trapped. We illustrate this problem in Fig. 9.

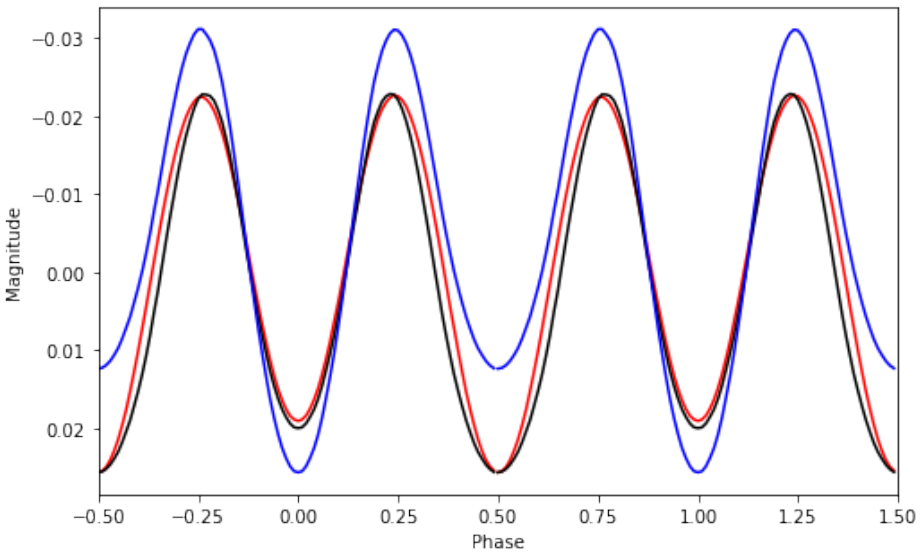

Figure 9: A comparison of the ellipsoidal variations of HD 74423 with theoretical fits. The red line is the average orbital light curve. In blue we show a model fit assuming no irradiation from the secondary star (cool secondary hypothesis), whereas the black line is a fit including the irradiation effect.

Evolutionary state of the system

The absence of the secondary in the spectra and our exercise of light curve modeling both suggest that the secondary is a faint, low-mass star. The spectroscopic analysis and the Spectral Energy Distribution (SED) fitting indicate the primary star is an evolved early A star. Based on these conclusions, we discuss the possible formation history of HD 74423.

First, the secondary star in the HD 74423 system could be a low-mass ($M \approx 0.2-0.5\,\mathrm{M}_{\odot}$) main-sequence star. This type of star would hardly move off the Zero-Age Main Sequence (ZAMS) during the lifetime of the Galaxy, and its radius essentially stays constant ($R \approx 0.2-0.5\,\mathrm{R}_{\odot}$). We would also expect its effective temperatures to be low ($T_{\rm eff} \approx 3200-3800\,\mathrm{K}$).

On the other hand, HD 74423 might belong to a class of binaries called EL CVn stars, which are composed of an F or A primary and a low-mass thermally bloated white dwarf (WD) secondary (e.g., KOI-81, ref.[36] and KIC 8262223, ref.[37]). This class of binary is formed from the evolution of two main-sequence star progenitors, through stable Roche Lobe Overflow (RLOF) mass transfer. Ref.[38] performed a binary population synthesis of EL CVn stars formed through RLOF. They found in EL CVn systems that the mass of the primary star ranges from 1.0 to $\approx 3.0\,\mathrm{M}_{\odot}$, and that of the He white dwarf ranges from 0.15 to $0.3\,\mathrm{M}_{\odot}$ (their fig. 14, 15; see also ref.[39]).

Interesting in this context is the λ Bootis-type spectral peculiarity of HD 74423. Despite many attempts, the cause of these peculiarities is still not fully understood. Several scenarios including accretion from protoplanetary disks, accretion from gas ablated from hot Jupiters, and interactions with diffuse interstellar clouds have been proposed (see ref.[40] for a discussion), but a combination of several of these channels is required to explain the λ Bootis

phenomenon as a whole. If the secondary star in the HD 74423 system were indeed a thermally bloated WD or proto-WD, one could speculate that mass transfer from a close binary companion could be responsible for the primary's λ Bootis-type abundance anomalies.

Summary and conclusions

We report the discovery of an oblique pulsation in the A star HD 74423 (TIC 355151781), aligned with the tidal bulge created by its binary companion. This star shows a single pulsation mode that generates a frequency multiplet split by the orbital frequency, and the frequency and phase patterns demonstrate that the pulsation axis lies near to the line of apsides. HD 74423 is the first obliquely pulsating star known where the location of the pulsation axis is dictated by the tidal distortion. Furthermore, and most interestingly, we show in this work that the star is almost exclusively pulsating in only one hemisphere. It remains unclear whether this is the hemisphere facing its companion or the one pointing away from it.

The pulsation mode in HD 74423 is currently unique, but there must be a class of such stars that have their pulsation axes aligned with their tidal axes, and this discovery is an impetus to search for more. It also motivates more detailed studies of the interaction between stellar pulsations and tidal distortion in binary stars. We know from the heartbeat stars that tides do excite modes that are nearly resonant with orbital harmonics. Although we do not have a statistical study yet, our own examination of *Kepler* and *TESS* data suggests that many close binary stars in the lower instability strip do not pulsate, yet some do. Do tides in binary stars impact the excitation of p modes and g modes? While this question remains a puzzle, HD 74423 and other stars like it (when they are found) may be the key.

The nature of the secondary star in the HD 74423 system is unclear. It could be either a normal main sequence star or a helium pre-white dwarf. In the latter case it could be hot enough to irradiate the gravity-darkened hemisphere of the primary, leading to an ambiguity regarding the hemisphere in which the pulsations are trapped. This problem can be resolved by obtaining a number of high-quality spectra over all orbital phases: the orbital radial velocity curve differs by 180° between the two scenarios. Efforts in this direction are underway.

References

[1] Balona, L. A., 1985 MNRAS 217, 17p

[2] Torres, G., Andersen, J., Giménez, A., 2010, A&ARv 18, 67

[3] Aerts, C., Christensen-Dalsgaard, J., & Kurtz, D. W., 2010, Asteroseismology, (Springer-Verlag, Berlin)

[4] Cowling, T. G., 1941, MNRAS 101, 367

[5] Handler, G., et al., 2002, MNRAS 333, 262

[6] Welsh, W. F., et al., 2011, ApJ 197, 4

[7] Thompson, S. E., et al., 2012, ApJ 753, 86

[8] Hambleton, K. M., et al., 2013, MNRAS 434, 925

[9] Hambleton, K. M., et al., 2018, MNRAS 473, 5165

[10] Kurtz, D. W., 1982, MNRAS 200, 807

[11] Ledoux, P., 1951, ApJ 114, 373

[12] Bigot, L., Kurtz, D. W., 2011, A&A 536, A73

[13] Pesnell W. D., 1985, ApJ, 292, 238

[14] Lenz P., 2011, in *New Horizons in Astronomy, Proceedings of the Frank N. Bash Symposium 2011*, ed. S. Salviander, J. Green & A. Pawlik, PoS 149, 3

[15] Houk, N., Cowley, A. P., 1975, *Michigan Spectral Catalogue*, Vol. 1

[16] Bernhard, K., Hümmerich, S., Otero, S., Paunzen, E., 2015, A&A 581, 138

[17] Pojmański, G. 2002, Acta Astron., 52, 397

[18] Gray R. O., Riggs Q. S., Koen C., Murphy S. J., Newsome I. M., Corbally C. J., Cheng K.-P., Neff J. E., 2017, AJ 154, 31

[19] Venn, K. A., Lambert, D. L., 1990, ApJ 363, 234

[20] Bohlender D. A., Landstreet J. D., 1990, MNRAS, 247, 606

[21] Kovács, G., Zucker, S., & Mazeh, T. 2002, A&A, 391, 369

[22] Rappaport, S., Vanderburg, A., Kristiansen, M. H., et al. 2019, MNRAS, 488, 2455

[23] Morris, S. L., 1985, ApJ, 295, 143

[24] Shibahashi, H., & Kurtz, D. W. 2012, MNRAS 422, 738

[25] Saio, H., & Gautschy, A. 2004, MNRAS, 350, 485

[26] Unno, W., Osaki, Y., Ando, H., et al. 1989, Nonradial oscillations of stars

[27] Flower, P. J., 1996, ApJ, 469, 355

[28] Livingston, W. C., 2000, in *Allen's Astrophysical Quantities*, 4$^{\rm th}$ edition, ed. A. N. Cox, Springer Verlag, p. 341

[29] Murphy, S. J., Hey, D., van Reeth, T., Bedding, T., 2019, MNRAS 485, 2380

[30] Paxton, B., Bildsten, L., Dotter, A., et al. 2011, ApJS 192, 3

[31] Asplund M., Grevesse N., Sauval A. J., Allende Prieto C., Kiselman D., 2004, A&A 417, 751

[32] Breger M., Bregman J. N., 1975, ApJ, 200, 343

[33] Fitch W. S., 1981, ApJ 249, 218

[34] Castelli, F., Kurucz, R. L. 2003, in IAU Symp. 210, Modelling of Stellar Atmospheres, ed. N. E. Piskunov, W. W. Weiss, & D. F. Gray (San Francisco, CA: ASP), A20

[35] Prša, A., Conroy, K. E., Horvat, M., Pablo, H., Kochoska, A., Bloemen, S., Giammarco, J., Hambleton, K. M., Degroote, P., 2016, ApJS 227, 29

[36] Matson, R. A., Gies, D. R., Guo, Z., Quinn, S. N., Buchhave, L. A., Latham, D. W., Howell, S. B., Rowe, J. F., 2015, ApJ 806, 155

[37] Guo, Z., Gies, D. R., Matson, R. A., Garcia Hernandez, A., Han, Z., Chen, X., 2017, ApJ 837, 114

[38] Chen, X., Maxted, P. F. L., Li, J., Han, Z., 2017, MNRAS 467, 1874

[39] Willems, B., Kolb, U., 2004, A&A 419, 1057

[40] Murphy, S. J., Paunzen, E., 2017, MNRAS 466, 546

[41] Lindegren, L., Hernandez, J, Bombrun, A., et al. 2018, arXiv:1804.09366.

[42] Skrutskie, M. F., Cutri, R. M., Stiening, R., et al. 2006, AJ, 131, 1163.

[43] Cutri, R.M., Wright, E.L., Conrow, T., et al. 2013, wise.rept, 1C.

Methods

Selection of interesting variable stars

For the searches of unusual variables in TESS data the visual surveyors utilized the `LcTools4` software[2] (ref.[1]).

Frequency analysis

The *TESS* data were analysed using a Discrete Fourier Transform (ref.[2]) to produce amplitude spectra.

[2]https://sites.google.com/a/lctools.net/lctools/

Spectroscopy and SED fitting

We observed HD 74423 spectroscopically using the 1.9-m telescope at the South African Astronomical Observatory (SAAO), Sutherland. We obtained six spectra on 3 different nights (2019 May 24, 25 and 27) using the "Spectrograph Upgrade: Newly Improved Cassegrain" (SpUpNIC) spectrograph. The high resolution blue grating 4 (G4) was used in each case and the exposure time was 400 s, resulting in signal-to-noise (S/N) ratios between $220-260$ per individual exposure. The effective resolution of the spectra is 2 Å, and the wavelength range covered 3740 – 4970 Å. We took Copper-Argon (CuAr) lamp spectra for wavelength calibration purposes. All spectra were reduced and continuum normalized using the available Image Reduction and Analysis Facility (IRAF) routines.

The spectra were analysed with the program `SPECTRUM` (ref.[3])[3] and ATLAS9 model atmospheres (ref.[4]). We fixed $\log g$ to 3.5 because our spectral resolution does not permit an independent determination. To determine the radial velocities of the star during the observations, we used a cross-correlation technique. We used the average spectrum of the star, each exposure shifted to zero radial velocity, as a template. The absolute values of the radial velocities were calculated by cross-correlating the template spectrum with a theoretical one computed with `SPECTRUM`. We found that using the metallic-line spectrum redward of 4200 Å gave the most reliable result.

We determined a $T_{\rm eff}$ value by fitting the Kurucz atmospheric models (ATLAS9 code, ref.[5]) to archive photometric colours given in Table 1. as well as BV (ref.[6]), and Galex[4] magnitudes and fluxes. In the analysis, we fixed $\log g = 3.5$ and assumed solar abundance, as SEDs depend only weakly on these parameters. $E(B-V) = 0.055$ was used to obtain the de-reddened SED during the analysis. The resulting $T_{\rm eff}$ was determined by minimizing the deviations between observations and fit. The uncertainty was estimated considering the errors in $E(B-V)$ of 0.02 mag, $\log g$ of 0.5, and [M/H] of 1 dex.

Modelling the ellipsoidal variations

We computed a series of model light curves using the `PHOEBE` code version 2.1.13 (refs.[7,8]) with fitting performed via a Markov Chain Monte Carlo (MCMC) method (as described by ref.[9]). The inclination and mass ratio were allowed to vary over a wide range while maintaining the properties of the primary within the uncertainties derived earlier.

References

[1] Kipping, D. M., Schmitt, A. R., Huang, X., Torres, G., Nesvorný, D., Buchhave, L. A., Hartman, J., Bakos, G. Á. 2015, ApJ, 813, 14

[2] Kurtz, D. W., 1985, MNRAS 213, 773

[3] Gray, R. O., Corbally, C. J., 1994, AJ, 107, 742

[3] http://www.appstate.edu/~grayro/spectrum/spectrum.html
[4] https://galex.stsci.edu/GR6/

[4] Castelli, F., Kurucz, R. L. 2003, in IAU Symp. 210, Modelling of Stellar Atmospheres, ed. N. E. Piskunov, W. W. Weiss, & D. F. Gray (San Francisco, CA: ASP), A20

[5] Kurucz, R., 1993, KurCD, 13

[6] Høg E., et al., 2000, A&A, 355, L27

[7] Prša, A., Conroy, K. E., Horvat, M., Pablo, H., Kochoska, A., Bloemen, S., Giammarco, J., Hambleton, K. M., Degroote, P., 2016, ApJS 227, 29

[8] Horvat, M., Conroy, K. E., Pablo, H., Hambleton, K. M., Kochoska, A., Giammarco, J., Prša, A., 2018, ApJS 237, 26

[9] Jones, D., Boffin, H. M. J., Sowicka, P., Miszalski, B., Rodríguez-Gil, P., Santander-García, M., Corradi, R. L. M., 2019, MNRAS 482, L75

Acknowledgments

This paper includes data collected by the *TESS* mission. Funding for the *TESS* mission is provided by the NASA Explorer Program. Funding for the *TESS* Asteroseismic Science Operations Centre is provided by the Danish National Research Foundation (Grant agreement no.: DNRF106), ESA PRODEX (PEA 4000119301) and Stellar Astrophysics Centre (SAC) at Aarhus University. DWK acknowledges financial support from the STFC via grant ST/M000877/1. MS is supported by an Australian Government Research Training Program (RTP) Scholarship. We thank the *TESS* team and staff and TASC/TASOC for their support of the present work. GH, SC, FKA and PS acknowledge financial support by the Polish NCN grant 2015/18/A/ST9/00578. We thank Allan R. Schmitt for making his light curve examining software `LcTools` freely available. SC is grateful to Chris Engelbrecht for introducing him to the use of the observing equipment. GH thanks Ernst Paunzen for helpful discussions on the spectra of λ Bootis stars.

Competing Interests

The authors declare that they have no competing financial interests.

Author contributions

GH provided the initial astrophysical interpretation for this object, coordinated the scientific analysis, analysed the spectroscopic data as well as oversaw and contributed to the paper writing. DWK carried out the frequency analysis and provided the interpretation in terms of the oblique pulsator model. SAR initiated the collaboration, oversaw and homogenized all aspects of the scientific analysis. HS modelled the pulsation amplitude and phase behaviour over the orbit. JF computed the MESA models. DJ and PS analysed the ellipsoidal variability. ZG discussed the evolutionary state of the system. SC carried out the spectroscopic observations and reduced them. FKA performed the SED fitting. MS and SJM independently noticed the star's behaviour and provided their expertise. RG and TLJ

originally pointed out the star to SAR and AV who work with the citizen scientists to vet their findings.

Correspondence

Correspondence and requests for materials should be addressed to Gerald Handler. (email: gerald@camk.edu.pl).